

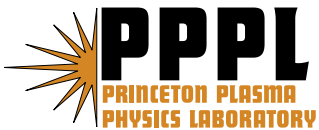
PPPL-4170

PPPL-4170

Two-stream Instability for a Longitudinally-compressing Charged Particle Beam

Edward A. Startsev and Ronald C. Davidson

June 2006



Princeton Plasma Physics Laboratory

Report Disclaimers

Full Legal Disclaimer

This report was prepared as an account of work sponsored by an agency of the United States Government. Neither the United States Government nor any agency thereof, nor any of their employees, nor any of their contractors, subcontractors or their employees, makes any warranty, express or implied, or assumes any legal liability or responsibility for the accuracy, completeness, or any third party's use or the results of such use of any information, apparatus, product, or process disclosed, or represents that its use would not infringe privately owned rights. Reference herein to any specific commercial product, process, or service by trade name, trademark, manufacturer, or otherwise, does not necessarily constitute or imply its endorsement, recommendation, or favoring by the United States Government or any agency thereof or its contractors or subcontractors. The views and opinions of authors expressed herein do not necessarily state or reflect those of the United States Government or any agency thereof.

Trademark Disclaimer

Reference herein to any specific commercial product, process, or service by trade name, trademark, manufacturer, or otherwise, does not necessarily constitute or imply its endorsement, recommendation, or favoring by the United States Government or any agency thereof or its contractors or subcontractors.

PPPL Report Availability

Princeton Plasma Physics Laboratory

This report is posted on the U.S. Department of Energy's Princeton Plasma Physics Laboratory Publications and Reports web site in Fiscal Year 2006.

The home page for PPPL Reports and Publications is:

http://www.pppl.gov/pub_report/

Office of Scientific and Technical Information (OSTI):

Available electronically at: <http://www.osti.gov/bridge>.

Available for a processing fee to U.S. Department of Energy and its contractors, in paper from:

U.S. Department of Energy
Office of Scientific and Technical Information
P.O. Box 62
Oak Ridge, TN 37831-0062

Telephone: (865) 576-8401

Fax: (865) 576-5728

E-mail: reports@adonis.osti.gov

Two-stream instability for a longitudinally-compressing charged particle beam*

Edward A. Startsev and Ronald C. Davidson

Plasma Physics Laboratory, Princeton University, Princeton, New Jersey 08543

The electrostatic two-stream instability for a cold, longitudinally-compressing charged particle beam propagating through a background plasma has been investigated both analytically and numerically. Small-signal coupled equations describing the evolution of the perturbations are derived, and the asymptotic solutions are obtained. The results are confirmed by direct numerical solution of the linearized fluid equations. It is found that the longitudinal beam compression strongly modifies the space-time development of the instability. In particular, the dynamic compression leads to a significant reduction in the growth rate of the two-stream instability compared to the case without an initial velocity tilt.

I. INTRODUCTION

To achieve the high focal spot intensities necessary for high energy density physics and heavy ion fusion applications, the ion beam pulse must be compressed longitudinally by factors of ten to one hundred before it is focused onto the target. The longitudinal compression is achieved by imposing an initial velocity profile tilt on the drifting beam in vacuum [1–3]. To achieve maximum longitudinal compression, the space charge of the beam is neutralized by propagation through a dense neutralizing background plasma [2–5]. If the space charge is fully neutralized by the plasma, the final compression is limited only by the initial longitudinal temperature of the beam ions and possible collective processes (such as the two-stream instability [6–9]) which may prevent full neutralization. The beam’s longitudinal thermal spread which could stabilize the instability also inhibits full longitudinal compression. Therefore, in this paper, we make use of macroscopic fluid model [10] to investigate both analytically and numerically the electrostatic two-stream instability for a cold, longitudinally-compressing charged particle beam propagating through a background plasma. It is found that the longitudinal beam compression alone strongly modifies the space-time development of the two-stream instability. In particular, it is found that the dynamic compression leads to a significant reduction in the growth rate of the two-stream instability compared to the case without an initial velocity tilt.

* Research supported by the U. S. Department of Energy.

The analysis presented here is similar to the analysis for a uniform infinite beam pulse [6]. In that case it is well known that the propagation of cold beam through a cold, background plasma is absolutely unstable. The effects that limit the the instability growth are the thermal spread of the beam particles and possible density gradients [11]. In the case considered here, the instability growth is limited by the velocity tilt. Indeed, for small beam density, the instability requires that the resonance condition $\omega = kV_b$ be satisfied for a continuous growth. Here ω_{pe} is the electron plasma frequency associated with the plasma electrons, k is the axial wavenumber of the perturbation, and V_b is the beam velocity. As shown in Section VI, the perturbation frequency changes with time due to the time-dependent beam velocity and beam density profile, and it eventually detunes out of resonance and the instability ceases. The present analysis takes into account the effects of the velocity tilt and allows the level of saturation to be determined. A similar analysis has been used to study the filamentation for a radially converging heavy ion beam [12]. The effects of radial convergence on the two-stream instability has also been studied [13, 14]. Numerical simulations using the particle-in-cell code LSP have recently appeared in the literature that address the practical requirements for neutralized propagation of heavy-ion beams for cases with and without longitudinal compression [3, 5]. Some preliminary numerical simulations of the possible effects of longitudinal compression on the two-stream instability for longitudinally-compressing heavy-ion beams have also been reported [3].

This paper is organized as follows. In Section II, we consider the unperturbed propagation of the electron beam in the background plasma. In Section III, small-signal equations are derived that describe the evolution of the density perturbations around the flow described by the unperturbed equations. In Section IV, we obtain the asymptotic solution of the resulting equations. In Section V, the development of the instability and its saturation are examined from the point of view of the wave dynamics, where the plasma waves are represented as quasi-particles characterized by their position $x(t)$, wavenumber $k(t)$ and energy (or frequency) $\omega(t)$. In Section VI, numerical solutions of the linearized equations are obtained and compared with the analytical results. Finally, the results are summarized in Sec. VII.

II. UNPERTURBED PROPAGATION

It is assumed that a semi-infinite electron beam with a sharp leading edge enters the chamber containing background plasma at time $t = 0$ and $x = 0$ with velocity V_b^0 and density n_b^0 . The beam is uniformly compressing in the longitudinal direction as it propagates inside the chamber

and reaches the maximum compression at time $t = T_f$ at the point $x = X_f = T_f V_b^0$ away from the beam entry point $x = 0$ into the chamber. The unperturbed beam propagation is illustrated in Fig. 1, where the beam phase space is plotted at different times during the compression. The transition from solid to dashed lines in Fig. 1 identifies the end of the real beam pulse with finite initial length L_b^0 . The frequently used parameter, the longitudinal "velocity tilt" $\Delta V_b^0/V_b^0$, is related to the compression distance X_f and the initial beam pulse length L_b^0 by

$$\Delta V_b^0/V_b^0 = L_b^0/X_f. \quad (1)$$

It is also assumed that the electron beam propagation in the background plasma is both charge neutralized and current neutralized, where the quasi-neutrality conditions are given by

$$\bar{n}_e + \bar{n}_b = n_0, \quad (2)$$

$$\bar{n}_e \bar{V}_e + \bar{n}_b \bar{V}_b = 0. \quad (3)$$

Here, \bar{n}_j and \bar{V}_j denote the dynamically changing unperturbed density and flow velocity of the beam electrons ($j=b$) and background plasma electrons ($j=e$), and $n_0 = \text{const.}$ (independent of x and t) is the uniform density of the background plasma ions (assumed singly-ionized). The quasi-neutrality condition is slightly violated due to the finite electron mass in the force balance equation for the plasma electrons

$$e\bar{E} = -m_e \left(\frac{\partial \bar{V}_e}{\partial t} + \bar{V}_e \frac{\partial \bar{V}_e}{\partial x} \right). \quad (4)$$

The zero-order solution for the beam density and velocity are given by

$$\bar{n}_b(t) = \frac{n_b^0 T_f}{T_f - t}, \quad (5)$$

$$\bar{V}_b(t, x) = \frac{V_b^0 T_f - x}{T_f - t}. \quad (6)$$

Here, it is also assumed that $\delta \equiv n_b^0/n_0 \ll 1$. Substituting Eqs. (2), (3) and (6) into Eq. (4), we obtain for the unneutralized electric field

$$e\bar{E} = 2m_e \frac{n_b^0}{n_0} \frac{(X_f - x)}{[(1 - t/T_f) + (n_b^0/n_0)]^2 T_f (T_f - t)}. \quad (7)$$

Using Poisson's equation $\partial \bar{E}/\partial x = 4\pi e \delta \bar{n} = 4\pi e (\delta \bar{n}_b - \delta \bar{n}_e)$, we obtain for the unneutralized charge density

$$\frac{\delta \bar{n}(x, t)}{\bar{n}_b(t)} = -\frac{2}{\omega_{pe}^2 T_f^2} \frac{1}{\left[\left(1 - \frac{t}{T_f} \right) + \frac{n_b^0}{n_0} \right]^2}, \quad (8)$$

where $\omega_{pe}^2 \equiv 4\pi n_0 e^2/m_e$ is the plasma frequency-squared of the background plasma electrons. In what follows we make use of two small parameters

$$\epsilon \equiv 1/(\omega_{pe} T_f) \ll 1 \quad \text{and} \quad \delta \equiv n_b^0/n_0 \ll 1. \quad (9)$$

It will be shown that the resonant two-stream instability develops and saturates everywhere in the chamber except close to the compression point $x = X_f$ during the time interval when $1-t/T_f \sim 1 \gg n_b^0/n_0$. It follows from Eq. (8) that $\delta \tilde{n}(x, t)/\bar{n}_b(t) \simeq 2\epsilon^2$ during this time interval and therefore for perturbations with amplitude $|\delta \tilde{n}(x, t)|/\bar{n}_b(t) \gg \epsilon^2$, the beam can be considered as fully neutralized by the background plasma.

III. SMALL-SIGNAL EQUATIONS

In this section, we derive the coupled equations that describe the perturbation in charge density of the beam electrons and background electrons. Quantities are expressed as $n_b = \bar{n}_b + \tilde{n}_b$, $v_b = \bar{V}_b + \tilde{v}_b$, $n_e = \bar{n}_e + \tilde{n}_e$, $v_e = \bar{v}_e + \tilde{v}_e$ where unperturbed quantities \bar{n}_b , \bar{V}_b , \bar{n}_e and \bar{V}_e are determined from Eqs. (2), (3), (5) and (6). Substituting Eqs. (5) and (6) into the linearized continuity equation for the beam particles, we obtain

$$(T_f - t) \frac{\partial \tilde{n}_b}{\partial t} - \tilde{n}_b + (T_f V_b^0 - x) \frac{\partial \tilde{n}_b}{\partial x} = -T_f n_b^0 \frac{\partial \tilde{v}_b}{\partial x}. \quad (10)$$

From the linearized momentum equation for the beam particles, we obtain

$$(T_f - t) \frac{\partial \tilde{v}_b}{\partial t} - \tilde{v}_b + (T_f V_b^0 - x) \frac{\partial \tilde{v}_b}{\partial x} = -\frac{e}{m_e} (T_f - t) \tilde{E}. \quad (11)$$

Here, E is linearized near $\bar{E} = 0$. Combining Eqs (10) and (11), and introducing the normalized variables,

$$t\omega_{pe} = \bar{t}, \quad x\omega_{pe}/V_b^0 = \bar{x}, \quad \tilde{n}_b/n_0 = \tilde{\tilde{n}}_b, \quad \tilde{v}_b/V_b^0 = \tilde{\tilde{v}}_b \quad \text{and} \quad e\tilde{E}/m_e\omega_{pe}V_b^0 = \tilde{\tilde{E}}, \quad (12)$$

we obtain

$$\begin{aligned} & [(1 - \epsilon\bar{t})\partial_{\bar{t}} + (1 - \epsilon\bar{x})\partial_{\bar{x}} - 2\epsilon][(1 - \epsilon\bar{t})\partial_{\bar{t}} + (1 - \epsilon\bar{x})\partial_{\bar{x}} - \epsilon]\tilde{\tilde{n}}_b \\ & = \alpha^2 \epsilon^2 (1 - \epsilon\bar{t})\partial_{\bar{x}} \tilde{\tilde{E}} = -\alpha^2 \epsilon^2 (1 - \epsilon\bar{t})(\tilde{\tilde{n}}_b + \tilde{\tilde{n}}_e), \end{aligned} \quad (13)$$

where $\alpha \equiv \omega_{pb} T_f$, and use has been made of Poisson's equation $\partial_{\bar{x}} \tilde{\tilde{E}} = -\tilde{\tilde{n}}_b - \tilde{\tilde{n}}_e$.

Repeating the same procedure for the background plasma electrons, we obtain

$$\begin{aligned} & [(1 - \epsilon\bar{t})(1 - \epsilon\bar{t} - \delta)\partial_{\bar{t}} - \delta(1 - \epsilon\bar{x})\partial_{\bar{x}} + 2\epsilon(1 - \epsilon\bar{t} + \delta)] \\ & \times [(1 - \epsilon\bar{t})(1 - \epsilon\bar{t} - \delta)\partial_{\bar{t}} - \delta(1 - \epsilon\bar{x})\partial_{\bar{x}} + \delta\epsilon]\tilde{\tilde{n}}_e \\ & = -(1 - \epsilon\bar{t} - \delta)^3 (1 - \epsilon\bar{t})(\tilde{\tilde{n}}_b + \tilde{\tilde{n}}_e) + 2\epsilon^2 \delta (1 - \epsilon\bar{t} - \delta). \end{aligned} \quad (14)$$

It will be shown later that the solutions to Eqs. (13) and (14) have the form $\tilde{n}_j = a_j \exp[-i(\bar{t} - \bar{x})]$, $j = b, e$, where the slowly varying amplitudes a_j satisfy $|\partial_{\bar{t}} a_j| \gg \delta |a_j|$. In this case we can neglect all terms that contain δ in Eq. (14). We also assume that the perturbation amplitude is larger than the unneutralized charge density ($\tilde{n}_e \gg \epsilon^2 \delta$) represented by the last term in Eq. (14) [see also Eq. (8)], and therefore the last term in Eq. (14) can be neglected. Hence, Eqs. (13) and (14) can be simplified to give

$$[(1 - \epsilon \bar{t}) \partial_{\bar{t}} + (1 - \epsilon \bar{x}) \partial_{\bar{x}} - 2\epsilon] [(1 - \epsilon \bar{t}) \partial_{\bar{t}} + (1 - \epsilon \bar{x}) \partial_{\bar{x}} - \epsilon] \tilde{n}_b = -\alpha^2 \epsilon^2 (1 - \epsilon \bar{t}) (\tilde{n}_e + \tilde{n}_b), \quad (15)$$

$$\partial_{\bar{t}}^2 \tilde{n}_e + \tilde{n}_e = -\tilde{n}_b. \quad (16)$$

Next, we change variables from \bar{x}, \bar{t} to

$$X = \epsilon \bar{x} \quad \text{and} \quad \tau = \bar{t} - \bar{x} \quad (17)$$

in Eqs. (15) and (16). With this change of variables, Eqs. (15) and (16) become

$$\begin{aligned} & [(1 - X) \partial_X - \tau \partial_\tau - 2] [(1 - X) \partial_X - \tau \partial_\tau - 1] \tilde{n}_b \\ & = -\alpha^2 (1 - X - \epsilon \tau) (\tilde{n}_e + \tilde{n}_b), \end{aligned} \quad (18)$$

$$(\partial_\tau^2 + 1) \tilde{n}_e = -\tilde{n}_b. \quad (19)$$

Substituting $\tilde{n}_j = a_j \exp[-i\tau]$, $j = e, b$, into Eqs. (18) and (19), for $\tau \gg 1$ we obtain the amplitude equation for a_e

$$[(1 - X) \partial_X + \tau(i - \partial_\tau)]^2 \partial_\tau (\partial_\tau - 2i) a_e = -\alpha^2 (1 - X - \epsilon \tau) (\partial_\tau - i)^2 a_e. \quad (20)$$

A similar equation can be obtained by substituting $kV_b = (\omega_p/V_b^0 - i\partial_x) \bar{V}_b(x, t)$ and $\omega = \omega_{pe} + i\partial_t$ into the two-stream dispersion relation for a beam-plasma system

$$\frac{\omega_{pe}^2}{\omega^2} + \frac{\omega_{pb}^2}{(\omega - kV_b)^2} = 1. \quad (21)$$

The resulting equation is

$$\begin{aligned} & \left[\frac{\partial}{\partial t} + V_b(x, t) \frac{\partial}{\partial x} + i \frac{\omega_{pe}}{V_b^0} [V_b(x, t) - V_b^0] \right]^2 \left(\frac{\partial a_e}{\partial t} - 2i\omega_{pe} \right) \frac{\partial a_e}{\partial t} = \\ & = -\omega_{pb}^2(x, t) \left(\frac{\partial a_e}{\partial t} - i\omega_{pe} \right)^2 a_e(x, t). \end{aligned} \quad (22)$$

Substituting Eqs. (5) and (6) into Eq. (22), we obtain Eq. (20). In the limit where $|\partial_X| \ll \tau$ and $|\partial_\tau| \ll 1$, Eq. (20) can be integrated to give

$$a_e = c(X) \exp \left(i\alpha^2 \frac{1 - X + \epsilon \tau \log(\epsilon \tau)}{2\tau} \right). \quad (23)$$

It will be shown later that $\partial_X \sim \alpha$, and therefore both conditions $|\partial_X| \ll \tau$ and $|\partial_\tau| \ll 1$ are equivalent to $\tau \gg \alpha$. To determine $c(X)$ in Eq. (23), we need to find a solution in the region $\tau \sim \alpha$ and then take the limit $\tau \gg \alpha$. In the region $\tau \sim \alpha$, we can neglect $\epsilon\tau \sim \delta^{1/2} \ll (1-X)$ in Eq. (18), which gives

$$[(1-X)\partial_X - \tau\partial_\tau - 2][(1-X)\partial_X - \tau\partial_\tau - 1]\tilde{n}_b = -\alpha^2(1-X)(\tilde{n}_e + \tilde{n}_b). \quad (24)$$

$$(\partial_\tau^2 + 1)\tilde{n}_e = -\tilde{n}_b. \quad (25)$$

IV. ASYMPTOTIC SOLUTION

We now introduce the variable $Y = \log[1/(1-X)]$, and carry out the integral transform of Eqs. (24) and (25) according to $\tilde{n}_e = \int_C ds \hat{n}_e(s, Y) \exp(-is\tau)$. This gives

$$[\partial_Y + s\partial_s - 1][\partial_Y + s\partial_s](1-s^2)\hat{n}_e = \alpha^2 \exp(-Y)s^2\hat{n}_e. \quad (26)$$

Here, use has been made of the fact that the integral transform of the operator $-\tau\partial_\tau \rightarrow \partial_s s = 1 + s\partial_s$. To solve Eq. (26), we introduce new variable $p = Y - \log(s) = \log[1/s(1-X)]$. In the new variables, Eq. (26) can be rewritten as

$$\partial_s^2 \hat{n}_b = \alpha^2 \frac{\exp(-p)}{s(1-s^2)} \hat{n}_b, \quad (27)$$

where use has been made of $\tilde{n}_b = -(\partial_\tau^2 + 1)\tilde{n}_e$, and therefore $\hat{n}_b = -(1-s^2)\hat{n}_e$. In obtaining Eqs. (26) and (27), it is assumed that the contour C is chosen so that the integrals exist and all integrand functions and their derivatives are zero on both ends of the contour C.

The WKB solution of Eq. (27) valid for $\alpha \gg 1$ is given by

$$\hat{n}_b = \bar{b}_\pm(p) \exp \left[\pm 2\alpha \exp(-p/2) \int_{\exp(-p/2)}^{\sqrt{s}} \frac{dz}{(1-z^4)^{1/2}} \right], \quad (28)$$

where $\bar{b}_\pm(p)$ are two arbitrary functions. Using Eq. (28), we can express the solution for \tilde{n}_b as

$$\tilde{n}_b = \sum_{\pm} \int_{C_{\pm}} ds f_{\pm}[s(1-X)] \exp \left[-i\tau s \pm 2\alpha s \sqrt{1-X} \int_{\sqrt{1-X}}^1 \frac{dz}{(1-s^2 z^4)^{1/2}} \right], \quad (29)$$

where the functions f_{\pm} and integration contours C_{\pm} are determined from the boundary conditions at $X = 0$. Taking the limit $X \rightarrow 0$ in Eq. (29), we obtain

$$\tilde{n}_b(\tau, 0) = \sum_{\pm} \int_{C_{\pm}} ds f_{\pm}(s) \exp(-i\tau s), \quad (30)$$

$$\partial_X \tilde{n}_b(\tau, 0) = \sum_{\pm} \int_{C_{\pm}} ds \left[-s f'_{\pm}(s) \pm \alpha \frac{s}{\sqrt{1-s^2}} f_{\pm}(s) \right] \exp(-i\tau s). \quad (31)$$

The boundary condition consistent with $\tilde{v}_b(\tau, X = 0) = 0$ that follow from Eq. (10) are

$$\tilde{n}_b(\tau, 0) = f(\tau)H(\tau), \quad (32)$$

$$\partial_X \tilde{n}_b(\tau, 0) = (1 + \tau \partial_\tau) \tilde{n}_b(\tau, 0), \quad (33)$$

where $H(\tau)$ is the Heaviside step-function defined by

$$H(\tau) = \begin{cases} 1 & \text{for } \tau \geq 1, \\ 0 & \text{for } \tau < 0. \end{cases} \quad (34)$$

Consistent with Eqs. (33) are the initial conditions and boundary conditions for the perturbed electron density, $\tilde{n}_e(\tau = 0) = \partial_\tau \tilde{n}_e(\tau = 0) = 0$ and $(\partial_\tau^2 + 1)\tilde{n}_e(\tau, X = 0) = -1$. The solution for \tilde{n}_b that satisfies the boundary conditions in Eq.(33) is given by

$$\tilde{n}_b = \int_{-\infty+i\Delta}^{+\infty+i\Delta} \frac{ds}{4\pi} \hat{f}[s(1-X)] \exp(-i\tau s) \sum_{\pm} \exp \left[\pm 2\alpha s \sqrt{1-X} \int_{\sqrt{1-X}}^1 \frac{dz}{(1-s^2 z^4)^{1/2}} \right], \quad (35)$$

where $\hat{f}(s) = \int_0^\infty d\tau \exp(is\tau) f(\tau)$, and Δ is such that integration contour in Eq. (35) is above all singularities of the function $\hat{f}(s)$.

Since $\alpha \gg 1$ is assumed, the integral in Eq. (35) can be evaluated using the method of steepest descend. First, we shift the integration contour into the lower half-plane. The resulting contour C' is shown in Fig. 2. The contour C' goes around the cuts and poles of the integrand in Eq. (35). The main contribution to the integral is from the points where the function

$$H_{\pm}(s) = -is \pm 2\beta s \sqrt{1-X} \int_{\sqrt{1-X}}^1 \frac{dz}{(1-s^2 z^4)^{1/2}} \quad (36)$$

reaches an extremum. Here, we also take the limit $\beta = \alpha/\tau \ll 1$, which allows determination of the extremum points analytically. The function $H_{\pm}(s)$ has root branch points at $s_b^I = \pm 1$ and $s_b^{II} = \pm 1/\sqrt{1-X}$, and is analytic everywhere in the complex s -plane with cuts made as shown in Fig. 2. The imaginary part of the functions H_{\pm} experience discontinuous jumps across the cuts. Equating the derivative to zero, $H'_{\pm}(s_0) = 0$, we find that the extremum points are located near the branch points. One can show that only the extremum points near $s_b = \pm 1$ give exponentially growing contributions to the integral in Eq. (36). Expanding the functions $H_{\pm}(s)$ near $s \approx \pm 1$ and keeping leading-order terms in the small parameter β , we obtain

$$\begin{aligned} H_+(s \simeq +1) &\simeq -is + \beta \sqrt{2(1-X)} F[\arccos(\sqrt{1-X})|1/2] - \beta \sqrt{2(1-X)} \sqrt{1-s}, \\ H_-(s \simeq -1) &\simeq -is + \beta \sqrt{2(1-X)} F[\arccos(\sqrt{1-X})|1/2] - \beta \sqrt{2(1-X)} \sqrt{1+s}, \end{aligned} \quad (37)$$

where $F(x|\alpha) = \int_0^x d\theta / \sqrt{1 - \alpha \sin^2 \theta}$ is a elliptic integral of the first kind.

From $H'_\pm(s_\pm^0) = 0$ we find that $s_+^0 = 1 + \beta^2(1 - X)/2$, which is located below the right cut, and $s_-^0 = -1 - \beta^2(1 - X)/2$, which is located above the left cut, as shown in Fig. 2. The corresponding extremum values of function $H_\pm(s_\pm^0)$ valid up to the second order in β are given by

$$H_\pm(s_\pm^0) = \mp i \left(1 - \frac{\beta^2(1 - X)}{2} \right) + \beta \sqrt{2(1 - X)} F[\arccos(\sqrt{1 - X})|1/2]. \quad (38)$$

With the same accuracy, it can be shown that, $1/\sqrt{-H''_+(s_+^0)} = -\beta\sqrt{1 - X} \exp(-i\pi/4)$ and $1/\sqrt{-H''_-(s_-^0)} = \beta\sqrt{1 - X} \exp(i\pi/4)$. The extra minus sign multiplies the contribution from s_+^0 because the integration contour direction is reversed at this point. For the simple boundary condition in Eq. (33), $f(\tau) = 1$, it follows that $\hat{f}(s) = i/s$ and we can express the asymptotic growing solution as

$$\begin{aligned} \tilde{n}_b(\tau, X) \simeq & \frac{\alpha}{\sqrt{2\pi\tau^3(1 - X)}} \sin[\tau - \alpha^2(1 - X)/2\tau + \pi/4] \\ & \times \exp \left\{ \alpha \sqrt{2(1 - X)} F[\arccos(\sqrt{1 - X})|1/2] \right\}. \end{aligned} \quad (39)$$

The easiest way to determine $\tilde{n}_e(\tau, X)$ is to solve the equation

$$(\partial_\tau^2 + 1)\tilde{n}_e(\tau, X) = -\tilde{n}_b(\tau, X) \quad (40)$$

with initial conditions $\tilde{n}_e(0, X) = 0$ and $\partial_\tau \tilde{n}_e(0, X) = 0$, and with $\tilde{n}_b(\tau, X)$ given by Eq. (39). In the limit $\alpha \gg 1$, the solution to Eq. (40) is given by

$$\begin{aligned} \tilde{n}_e(\tau, X) \simeq & \frac{1}{2(1 - X)} \operatorname{Re} \left\{ \exp(i\tau) \left(1 - \operatorname{Erf} \left[\sqrt{\frac{i\alpha^2(1 - X)}{2\tau}} \right] \right) \right\} \\ & \times \exp \left\{ \alpha \sqrt{2(1 - X)} F[\arccos(\sqrt{1 - X})|1/2] \right\}, \end{aligned} \quad (41)$$

where $\operatorname{Erf}[x]$ is the error function defined by $\operatorname{Erf}[x] = 2/\sqrt{\pi} \int_0^x dx \exp(-x^2)$. The solutions in Eqs. (39) and (41) are valid far enough away from the beam head that $\tau \gg \alpha\sqrt{1 - X}$. At the end of the compression, $t = T_f$ and $\tau = \alpha^2(1 - X)$. At this time, the density perturbation can be expressed as

$$\tilde{n}_b(t = T_f, X) \simeq q_b \frac{\exp G(X)}{\alpha^2(1 - X)^2} \sin[\alpha^2(1 - X) + \pi/4 - \phi_b], \quad (42)$$

$$\tilde{n}_e(t = T_f, X) \simeq q_e \frac{\exp G(X)}{(1 - X)} \sin[\alpha^2(1 - X) + \pi/4 - \phi_e], \quad (43)$$

where the gain function $G(x)$ is defined by

$$G(X) = \alpha \sqrt{2(1 - X)} F[\arccos(\sqrt{1 - X})|1/2]. \quad (44)$$

In Eqs. (42) and (43) $q_b = 1/\sqrt{2\pi} \approx 0.40$, $\phi_b = 1/2$, and $q_e \exp[-i(\phi_e + \pi/4)] = (1 - \operatorname{Erf}[\sqrt{i/2}])/2$. Numerically, we find $q_e \approx 0.29$ and $\phi_e \approx 0.12$.

V. PHYSICAL DISCUSSION

As evident from Eqs. (42)–(43), the saturated amplitude of the density perturbations is determined mostly by the gain function in Eq. (44). It is interesting to examine the development of the instability and its saturation from the point of view of wave dynamics where the plasma waves are represented as quasi-particles characterized by their position $x(t)$, wave-number $k(t)$ and energy (or frequency) $\omega(t)$. The quasi-particle dynamics are described by the equations

$$\frac{dx}{dt} = \frac{\partial\omega}{\partial k} = -\frac{\partial D/\partial k}{\partial D/\partial w}, \quad (45)$$

$$\frac{dk}{dt} = -\frac{\partial\omega}{\partial x} = \frac{\partial D/\partial x}{\partial D/\partial w}, \quad (46)$$

$$\frac{d\omega}{dt} = \frac{\partial\omega}{\partial t} = -\frac{\partial D/\partial t}{\partial D/\partial w}, \quad (47)$$

where, for a beam propagating through background plasma, the dispersion function D is defined by

$$D = 1 - \frac{\omega_{pe}^2}{\omega^2} - \frac{\omega_{pb}^2(t)}{(\omega - kV_b(x, t))^2}, \quad (48)$$

and the quasi-particle dynamics is on the surface $D = 0$. Substituting Eq. (48) into Eqs. (45)–(47), we obtain the closed system of equations for $x(t)$ and $p(t) = k(t)V_b(x, t)/\omega(t)$

$$\frac{dx}{dt} = \frac{V_b(x, t)}{1 + (1 - p)^3/\delta(t)}, \quad (49)$$

$$\frac{dp}{dt} = \left[p - \frac{p^2}{1 + (1 - p)^3/\delta(t)} \right] \frac{1}{V_b(x, t)} \frac{\partial V_b(x, t)}{\partial t} - \left[\frac{p(1 - p)/2}{1 + (1 - p)^3/\delta(t)} \right] \frac{1}{\delta(t)} \frac{\partial \delta(t)}{\partial t}, \quad (50)$$

where $\delta(t) = \omega_{pb}^2(t)/\omega_{pe}^2$, and

$$\frac{\omega}{\omega_{pe}} = \left[1 + \frac{1}{(1 - p)^2/\delta(t)} \right]^{1/2}. \quad (51)$$

It follows from Eq. (51) that for $\delta \ll 1$ the maximum growth rate occurs for $p \sim 1$, which corresponds to perfect resonance. Equation (50) describes the detuning from resonance for particular quasi-particle under consideration. For a uniform non-compressing beam with $V_b = \text{const.}$, Eqs. (49) and (50) are easily solved to give

$$p = p_0, \quad (52)$$

$$x - \frac{V_b t}{1 + (1 - p)^3/\delta} = x_0, \quad (53)$$

with general solution $p(x, t)$ given by

$$x - \frac{V_b t}{1 + (1 - p)^3/\delta} = f(p). \quad (54)$$

We are interested in obtaining self-similar solutions which correspond to asymptotic solutions independent of the initial conditions. Such a solution is given by

$$(1-p)^3 = \delta \left[\frac{V_b t - x}{x} \right]. \quad (55)$$

For $\delta^{1/3}[x/(V_b t - x)]^{2/3} \ll 1$, we obtain from Eq. (51)

$$\frac{\omega}{\omega_{pe}} = 1 + \frac{(i\sqrt{3}-1)\delta^{1/3}}{2} \left[\frac{x}{V_b t - x} \right]^{2/3}, \quad (56)$$

where only the unstable solution with positive imaginary part of the frequency is retained. From Eq. (56), we obtain the gain function

$$G(x, t) = \int_{x/V_b}^t \text{Im}\omega(x, \bar{t}) d\bar{t} = \frac{3\sqrt{3}\omega_{pe}}{4V_b} \delta^{1/3} x^{2/3} (V_b t - x)^{1/3}. \quad (57)$$

The gain function in Eq. (57) coincides with the gain function obtained by direct solution of the linearized fluid equations [6]. It follows from Eq. (57) that the gain function never saturates. This is because the quasi-particle's detuning $p-1$ does not change with time [see Eq. (52)], and quasi-particles which were in resonance will stay in resonance indefinitely.

For the case where the beam velocity $V_b(x, t)$ changes dynamically according to Eq. (6), it follows that Eqs. (49) and (50) become

$$\frac{dp}{dT} = p - \frac{p(1+p)/2}{1+(1-p)^3/\delta}, \quad (58)$$

$$\frac{dY}{dT} = \frac{1}{1+(1-p)^3/\delta}, \quad (59)$$

where $Y = \log[1/(1-x/X_f)]$ and $T = \log[1/(1-t/T_f)]$. Introducing q defined by $p = 1 + q\delta^{1/3}$ in Eq. (50), we obtain equations for q valid to leading order in the small parameter δ , i. e.,

$$\delta^{1/3} \left(\frac{dq}{dT} + \frac{5}{6}q \right) = -q^3, \quad (60)$$

$$\frac{d\xi}{dT} = -q^3, \quad (61)$$

$$\frac{\omega}{\omega_{pe}} = \hat{\omega} = \left[1 + \frac{\delta^{1/3}}{q^2} \right]^{1/2}, \quad (62)$$

where $\xi = T - Y$. As shown below, the instability in this case saturates when $q \sim \delta^{1/6} \ll 1$, which justifies retaining only leading-order terms in Eqs. (60) and (61). The solution to Eqs. (60) and (61) is given by

$$\exp(-2T) \left[\frac{\delta^{1/3}(T)}{q^2} + 1 \right] = I. \quad (63)$$

$$\xi = \xi_0 - \delta(T)^{1/2} \int_0^T d\bar{T} \frac{\exp[(\bar{T}-T)/2]}{[\exp(2\bar{T})I - 1]^{3/2}}, \quad (64)$$

where I and ξ_0 are invariants of the motion. Making use of Eqs. (62), (63) and (64), we obtain the asymptotic solution for $\hat{\omega}(\xi, T) = \omega/\omega_{pe}$, which is independent on initial conditions, i. e.,

$$\xi = -2\delta(T)^{1/2} \int_{\exp(-T/2)}^1 \frac{d\eta}{[\eta^4 \hat{\omega}^2 - 1]^{3/2}}. \quad (65)$$

The gain function $G(x, t)$ is given by

$$G(x, t) = \int_{x/V_b}^t Im\omega(x, \bar{t}) d\bar{t} = \omega_{pe} T_f \exp(-Y) Im \int_0^\xi d\bar{\xi} \exp(-\bar{\xi}) \hat{\omega}(\bar{\xi}, Y). \quad (66)$$

It can be shown from Eq. (65) that $Im\hat{\omega} \sim (\delta)^{3/2}/\xi^3$ for $\xi/\delta^{1/2} \gg 1$ so that we can neglect the exponential contribution in Eq. (66) to the integral, and also extend the upper integration limit to infinity for $\xi \gg \delta^{1/2}$. In addition, we can also replace $T \rightarrow Y$ on the right-hand side of Eq. (65). Integrating Eq. (66) by parts and taking into account that $Im[\hat{\omega}(\xi)]\xi \sim 1/\xi^2 \rightarrow 0$ for $\xi \rightarrow \infty$, and $Im[\hat{\omega}(\xi)]\xi \sim \xi^{2/3} \rightarrow 0$ for $\xi \rightarrow 0$, we obtain

$$\begin{aligned} G &= \omega_{pe} T_f \exp(-Y) Im \int_0^\infty d\xi \hat{\omega}(\xi, Y) = -\omega_{pe} T_f \exp(-Y) Im \int_{\hat{\omega}(0, Y)}^{\hat{\omega}(\infty, Y)} d\hat{\omega} \xi(\hat{\omega}, Y) \\ &= -2\alpha \sqrt{1-X} Im \int_{\sqrt{1-X}}^1 \frac{d\eta}{\sqrt{\eta^4 - 1/\hat{\omega}^2}} \Big|_{\hat{\omega}(0, Y)}^{\hat{\omega}(\infty, Y)}, \end{aligned} \quad (67)$$

where $\alpha = \delta_0^{1/2} \omega_{pe} T_f = \omega_{pb} T_f$. Equation (65) has several solutions. The solution with positive imaginary part to the frequency, which corresponds to instability, corresponds to $\hat{\omega}^2(\infty, Y) = 1$ and $\hat{\omega}^2(0, Y) = \infty$. Therefore, using Eq. (67), we obtain

$$G(X) = 2\alpha \sqrt{1-X} \int_{\sqrt{1-X}}^1 \frac{d\eta}{\sqrt{1-\eta^4}} = \alpha \sqrt{2(1-X)} F[\arccos(\sqrt{1-X})|1/2], \quad (68)$$

where $X = x/X_f$. The gain function in Eqs. (68) is identical to Eq. (44). The region where it is valid, $\xi \gg \delta^{1/2}$ or $\tau = \omega_p(t - x/V_b) \gg \alpha \sqrt{1-x/X_f}$, also coincides with region where Eq. (44) is valid. The fact that we have obtained identical expressions for the gain function demonstrates the consistency of the approximations used in the derivations. The method of quasi-particles also clarifies the dynamics of the instability in physically intuitive way.

VI. NUMERICAL SOLUTION

As anticipated in Eq. (23), the amplitude $c(X) = |a_e| = \exp(G)$ is primarily a function of X and satisfies $\partial_X \sim \alpha$. The gain function can be expressed as

$$G(X) = \alpha \sqrt{2(1-X)} F[\arccos(\sqrt{1-X})|1/2]. \quad (69)$$

To check the approximations, we have solved the linearized system of equations in Eqs. (13) and (14) numerically using the FEMLAB package [15]. For the numerical analysis the parameters are taken to be $\epsilon = 1/(\omega_{pe}T_f) = 10^{-3}$ and $\delta = n_b^0/n_0 = 10^{-3}$. These parameters correspond to $\alpha^2 = \delta/\epsilon^2 = (\omega_{pb}T_f)^2 = 1000$. To compare with the theoretical results in Secs. IV and V, $f(\tau) = 1$ is chosen for the boundary conditions in Eqs. (33). The numerical results are shown in Figs. 3–7. Figure 3 shows the logarithm of the electron density perturbation, $\log|\tilde{n}_e|$, at time $t = 0.85T_f$ plotted as a function of the distance $X = x/X_f$. The lower (red) curve in Fig. 3 is the numerical solution of the linearized fluid equations with no approximations. The upper (blue) curve in Fig. 3 is the numerical solution of the same equations with the approximation $(1 - X - \epsilon\tau) \rightarrow (1 - X)$ on the right-hand side of Eq. (19). As evident from Fig. 3, this approximation does not change the space-time dependence of the solution, but only changes the overall amplitude slightly. Figure 4 illustrates the time dependence of the electron density perturbation $\log|\tilde{n}_e(X, \tau)|$. The logarithm of the electron density perturbation $\log|\tilde{n}_e|$ is plotted as a function of distance x/X_f at different times (1) $t/T_f = 0.25$, (2) 0.35, (3) 0.45, (4) 0.55, (5) 0.65, (6) 0.75, and (7) 0.85. It is evident from the Fig. 4 that the amplitude, $|\tilde{n}_e(X, \tau)|$, is indeed only a function of X away from the beam head where $\tau > \alpha\sqrt{1 - X}$. Figure 5 shows the logarithm of the electron density perturbation, $\log|\tilde{n}_e|$, plotted as a function of distance $X = x/X_f$ at $t = 0.85T_f$ obtained numerically and compared with the analytical solution in Eq. (68). As evident from Fig. 5, the agreement is very good. The gain function in Eq. (69) scales linearly with parameter $\alpha = \omega_{pb}T_f$. This scaling is confirmed in Fig. 6 where the logarithm of the electron density perturbation, $\log|\tilde{n}_e|$, is plotted as a function of distance $X = x/X_f$ at $t = 0.80T_f$, together with the analytical solution for the case where the beam density is reduced by a factor of four ($\alpha^2 = 250$) compared to the case shown in Fig. 5. Figure 7 shows a comparison of the gain function in Eq. (68) with the gain function for a beam with zero velocity tilt [Eq. (70)], i.e.,

$$G_{notilt}(X, t = T_f) = \alpha \frac{3\sqrt{3}}{4} \frac{X^{2/3}(1 - X)^{1/3}}{\delta^{1/6}}. \quad (70)$$

As evident from Fig. 7, for $\delta^{1/6} \ll 1$ the velocity tilt significantly reduces the growth rate compared to the case of a beam with zero initial velocity tilt.

VII. CONCLUSIONS

The electrostatic two-stream instability for a cold, longitudinally-compressing electron beam propagating through a background plasma has been investigated both analytically and numeri-

cally. Small-signal coupled equations describing the evolution of the density perturbations were derived, and the asymptotic solutions were obtained. The results were confirmed by direct numerical solution of the linearized fluid equations. It was shown that the longitudinal beam compression strongly modifies the space-time development of the instability. In particular, the dynamic compression leads to a significant reduction in the growth rate of the two-stream instability compared to the case without an initial velocity tilt by a factor $G_{max}/G_{max}^{notilt} \sim (\omega_{pb}/\omega_{pe})^{1/3} \ll 1$. The number of e-foldings is proportional to the number of beam-plasma periods $1/\omega_{pb}$ during the compression time T_f . The two-stream instability is completely mitigated by the effects of dynamical beam compression when $\omega_{pb}T_f \lesssim 1$.

In the present, we considered the case of a semi-infinite beam [see Fig. 1]. For a beam with finite initial length L_b^0 , the trailing beam end will trace the trajectory $x_{end}(t) = V_b^0 t [1 + L_b^0/X_f] - L_b^0$. In this case, the present analysis is applicable everywhere between the leading and trailing edges of the beam, $\max\{0, x_{end}(t)\} \leq x \leq x_{head}(t) = V_b^0 t$, where the beam can drive the background plasma unstable. Behind the beam, for $0 \leq x < x_{end}(t)$ the plasma will be left with remnant collective oscillations with constant amplitude, which are excited by the propagating beam.

The full neutralization assumption is also violated at the beam head, where the time-changing magnetic field induces a longitudinal electric field which acts on the plasma electrons to cause a flow of return current opposite to the injected current. The distance from the beam head where the current and charge neutrality conditions are violated depends on the smoothness of the beam head density profile [16]. Generally, if the density profile of the beam increases from zero to its maximum value over a distance larger than V_{b0}/ω_{pe} , the the beam charge is fully neutralized. In addition, the beam current will be neutralized if the beam diameter is much larger than the collisionless skin-depth c/ω_{pe} .

In this paper, we considered only low-density electron beam propagation in a background plasma. In this case, the unstable interaction is between the beam electrons and the plasma electrons. In the general case of a beam with arbitrary charge species and mass, the instability may also involve the background plasma ions, because of the non-zero relative velocity between the background ions and the neutralizing plasma electrons. This will occur if the beam ions are sufficiently heavy that the beam plasma frequency is smaller than the background ion plasma frequency, $\omega_{pb} \ll \omega_{pi}$. In this case, the two-stream instability between the background plasma electrons and the background plasma ions is expected to lead to a heating of the background electrons to thermal velocities comparable with the average flow velocity of the neutralizing background electrons $\sim (n_b/n_e)V_b$. During this initial stage, the beam ions are relatively unaffected. At later times, a

two-stream instability between the beam ions and the (heated) background electrons may develop. This later stage of instability, which directly effects the beam particles, can also be described by analysis presented in this paper.

ACKNOWLEDGMENT

This research was supported by the U. S. Department of Energy.

REFERENCES

- [1] E. A. Startsev and R. C. Davidson, *New Journal of Physics* **6**, 141 (2004).
- [2] P. K. Roy, S. S. Yu, E. Henestroza *et al.*, *Phys. Rev. Lett.* **95**, 234801 (2005).
- [3] D. R. Welch, D. V. Rose, T.C. Genoni, S. S. Yu and J. J. Barnard, *Nucl. Instrum. Methods Phys. Res. A* **544**, 236 (2005).
- [4] P. K. Roy S. S. Yu, S. Eylon *et al.*, *Phys. Plasmas* **11**, 2890 (2004).
- [5] C. Thoma, D. R. Welch, S. S. Yu, E. Henestroza, P. K. Roy, S. Eylon, and E. P. Gilson, *Phys. Plasmas* **12**, 043102 (2005).
- [6] R. Briggs, in *Advances in Plasma Physics*, edited by A. Symon and W. B. Thompson (Interscience, New York, 1971), Vol. 4, p.43.
- [7] R. C. Davidson, I. Kaganovich, H. Qin, E. A. Startsev, D. R. Welch, D. V. Rose, and H. S. Uhm, *Phys. Rev. ST Accel. Beams*, **7**, 114801, (2004).
- [8] H. Qin, E. A. Startsev and R. C. Davidson, *Physical Review Special Topics on Accelerators and Beams* **6**, 014401 (2003).
- [9] H. Qin, *Physics of Plasmas* **10**, 2708 (2003).
- [10] R. C. Davidson and H. Qin, *Physics of Intense Charged Particle Beams in High Energy Accelerators* (World Scientific, Singapore, 2001), and references therein.
- [11] D. D. Ryutov, *Sov. Phys.-JETP* **30**, 131 (1970).
- [12] E. P. Lee, Simon Yu, H. L. Buchanan, F. W. Chambers and M. N. Rosenbluth, *Phys. Fluids* **23**, 2095 (1980).
- [13] T. C. Genoni, D. V. Rose, D. R. Welch and E. R. Lee, *Phys. Plasmas* **11**, L73 (2004).
- [14] P. Stroud, *Laser and Particle Beams* **4**, 261 (1986).
- [15] FEMLAB Reference Manual, Comsol AB, Stockholm, Sweden, version 2.2 ed. (2001).
- [16] I. Kaganovich, E. A. Startsev and R. C. Davidson, *Phys. Plasmas* **11**, 3546 (2004).

FIGURE CAPTIONS

Fig.1 : Plot of the beam phase space at different times during the compression. Line 1 corresponds to $t = 0$.

Fig.2 : Integration contour and location of extremum points for the functions $H_{\pm}(s)$ in Eq. (36).

Fig.3 (Color online): Logarithm of the electron density perturbation $\log |\tilde{n}_e|$ at time $t = 0.85T_f$ plotted as a function of distance $X = x/X_f$. The lower (red) curve in is the numerical solution of the linearized fluid equations with no approximations and the upper (blue) curve is the numerical solution of the same equations with the approximation $(1 - X - \epsilon\tau) \rightarrow (1 - X)$ on the right-hand side of Eq. (19).

Fig.4 : Logarithm of the electron density perturbation $\log |\tilde{n}_e|$ plotted as a function of distance x/X_f at different times $t/T_f = 0.25$ (1), 0.35 (2), 0.45 (3), 0.55 (4), 0.65 (5), 0.75 (6), and 0.85 (7).

Fig.5 (Color online): Logarithm of the electron density perturbation $\log |\tilde{n}_e|$ plotted as a function of distance x/X_f at $t = 0.85T_f$ obtained numerically (solid curve) and compared with the analytical result in Eq. (69) (dashed curve).

Fig.6 (Color online): Logarithm of the electron density perturbation $\log |\tilde{n}_e|$ plotted as a function of distance x/X_f at $t = 0.80T_f$ obtained numerically (solid curve) and compared with the analytical result in Eq. (69) (dashed curve) for $\alpha^2 = 250$.

Fig.7 : Comparison of the instability gain as a function of x/X_f for a beam with (solid curve) and without (dashed curve) velocity tilt for $\delta = n_b^0/n_0 = 10^{-3}$ and $\alpha^2 = (\omega_{pb}T_f)^2 = 1000$.

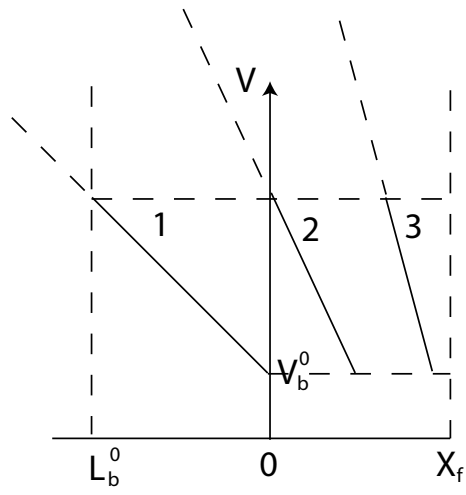


FIG. 1:

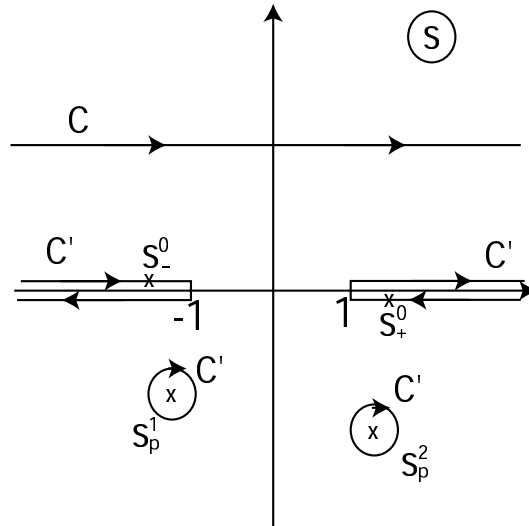


FIG. 2:

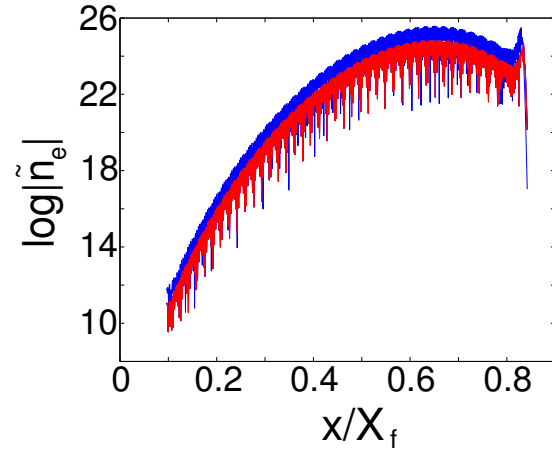


FIG. 3:

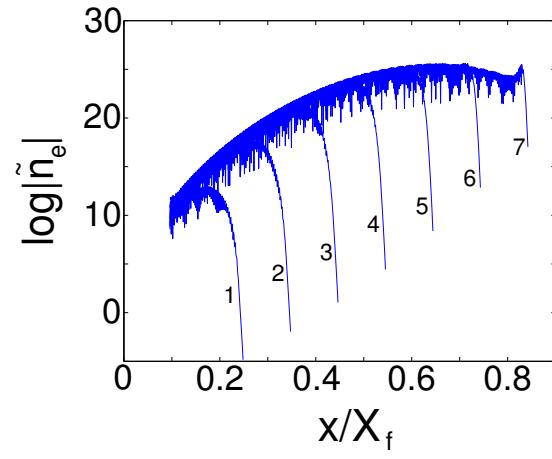


FIG. 4:

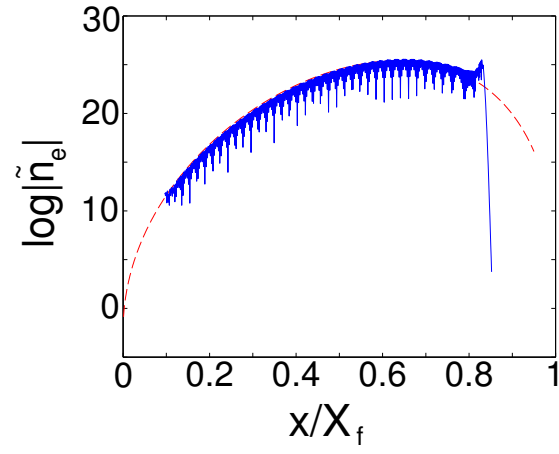


FIG. 5:

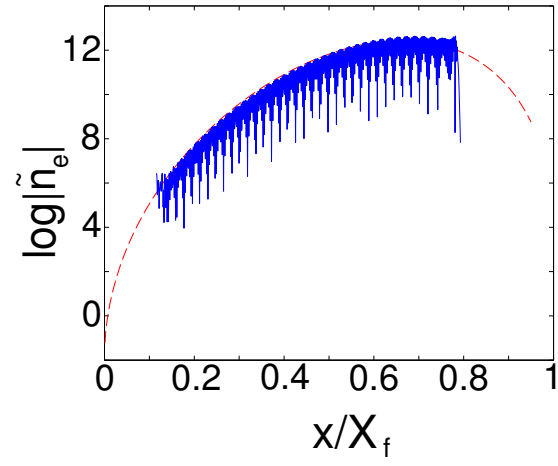


FIG. 6:

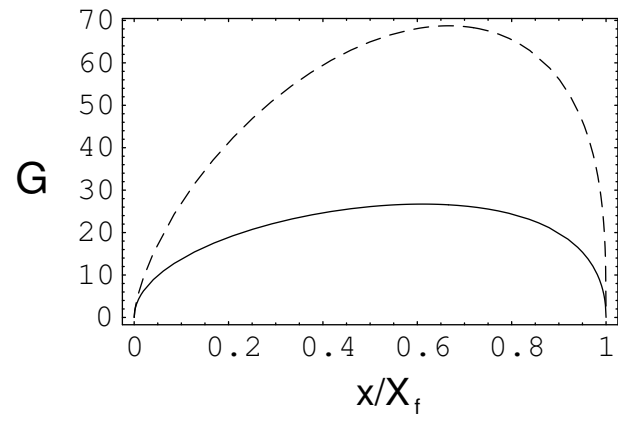


FIG. 7:

External Distribution

Plasma Research Laboratory, Australian National University, Australia
Professor I.R. Jones, Flinders University, Australia
Professor João Canalle, Instituto de Fisica DEQ/IF - UERJ, Brazil
Mr. Gerson O. Ludwig, Instituto Nacional de Pesquisas, Brazil
Dr. P.H. Sakanaka, Instituto Fisica, Brazil
The Librarian, Culham Science Center, England
Mrs. S.A. Hutchinson, JET Library, England
Professor M.N. Bussac, Ecole Polytechnique, France
Librarian, Max-Planck-Institut für Plasmaphysik, Germany
Jolan Moldvai, Reports Library, Hungarian Academy of Sciences, Central Research
Institute for Physics, Hungary
Dr. P. Kaw, Institute for Plasma Research, India
Ms. P.J. Pathak, Librarian, Institute for Plasma Research, India
Dr. Pandji Triadyaksa, Fakultas MIPA Universitas Diponegoro, Indonesia
Professor Sami Cuperman, Plasma Physics Group, Tel Aviv University, Israel
Ms. Clelia De Palo, Associazione EURATOM-ENEA, Italy
Dr. G. Grosso, Istituto di Fisica del Plasma, Italy
Librarian, Naka Fusion Research Establishment, JAERI, Japan
Library, Laboratory for Complex Energy Processes, Institute for Advanced Study,
Kyoto University, Japan
Research Information Center, National Institute for Fusion Science, Japan
Professor Toshitaka Idehara, Director, Research Center for Development of Far-Infrared Region,
Fukui University, Japan
Dr. O. Mitarai, Kyushu Tokai University, Japan
Mr. Adefila Olumide, Ilorin, Kwara State, Nigeria
Dr. Jiangang Li, Institute of Plasma Physics, Chinese Academy of Sciences, People's Republic of China
Professor Yuping Huo, School of Physical Science and Technology, People's Republic of China
Library, Academia Sinica, Institute of Plasma Physics, People's Republic of China
Librarian, Institute of Physics, Chinese Academy of Sciences, People's Republic of China
Dr. S. Mirnov, TRINITI, Troitsk, Russian Federation, Russia
Dr. V.S. Strelkov, Kurchatov Institute, Russian Federation, Russia
Kazi Firoz, UPJS, Kosice, Slovakia
Professor Peter Lukac, Katedra Fyziky Plazmy MFF UK, Mlynska dolina F-2, Komenskeho Univerzita,
SK-842 15 Bratislava, Slovakia
Dr. G.S. Lee, Korea Basic Science Institute, South Korea
Dr. Rasulkhozha S. Sharafiddinov, Theoretical Physics Division, Institute of Nuclear Physics, Uzbekistan
Institute for Plasma Research, University of Maryland, USA
Librarian, Fusion Energy Division, Oak Ridge National Laboratory, USA
Librarian, Institute of Fusion Studies, University of Texas, USA
Librarian, Magnetic Fusion Program, Lawrence Livermore National Laboratory, USA
Library, General Atomics, USA
Plasma Physics Group, Fusion Energy Research Program, University of California at San Diego, USA
Plasma Physics Library, Columbia University, USA
Alkesh Punjabi, Center for Fusion Research and Training, Hampton University, USA
Dr. W.M. Stacey, Fusion Research Center, Georgia Institute of Technology, USA
Director, Research Division, OFES, Washington, D.C. 20585-1290

The Princeton Plasma Physics Laboratory is operated
by Princeton University under contract
with the U.S. Department of Energy.

Information Services
Princeton Plasma Physics Laboratory
P.O. Box 451
Princeton, NJ 08543

Phone: 609-243-2750
Fax: 609-243-2751
e-mail: pppl_info@pppl.gov
Internet Address: <http://www.pppl.gov>